

# Analysis of *NUAK1* and *NUAK2* expression during early chick development reveals specific patterns in the developing head

ABDELHAMID BEKRI<sup>#</sup>, MARC BILLAUD and JACQUES THÉLU\*

Univ. Grenoble Alpes, INSERM, CNRS, France

**ABSTRACT** Several human diseases are associated with the *NUAK1* and *NUAK2* genes. These genes encode kinases, members of the AMPK-related kinases (ARK) gene family. Both *NUAK1* and *NUAK2* are known targets of the serine threonine kinase LKB1, a tumor suppressor involved in regulating cell polarity. While much is known about their functions in disease, their expression pattern in normal development has not been extensively studied. Here, we present the expression patterns for *NUAK1* and *NUAK2* in the chick during early-stage embryogenesis, until day 3 (Hamburger and Hamilton stage HH20). Several embryonic structures, in particular the nascent head, showed distinct expression levels. *NUAK1* expression was first detected at stage HH6 in the rostral neural folds. It was then expressed (HH7-11) throughout the encephalon, predominantly in the telencephalon and mesencephalon. *NUAK1* expression was also detected in the splanchnic endoderm area at HH8-10, and in the vitellin vein derived from this area, but not in the heart. *NUAK2* expression was first detected at stage HH6 in the neural folds. It was then found throughout the encephalon at stage HH20. Particular attention was paid in this study to the dorsal ectoderm at stages HH7 and HH8, where a local deficit or accumulation of *NUAK2* mRNA were found to correlate with the direction of curvature of the neural plate. This is the first description of *NUAK1* and *NUAK2* expression patterns in the chick during early development; it reveals non-identical expression profiles for both genes in neural development.

**KEY WORDS:** *NUAK*, chick embryo, *in situ* hybridization

*NUAK1* and *NUAK2* are members of the novel (*Nua*) kinases family. Their alternative names include: *ARK5* or *OMPHK1* for *NUAK1*; and *SNARK* or *OMPHK2* for *NUAK2*. They are two of the fourteen known substrates of the serine threonine kinase LKB1 and are part of the AMPK-related protein kinase family (ARK) (Al-Hakim *et al.*, 2005, Hardie and Alessi, 2013, Manning *et al.*, 2002, Suzuki *et al.*, 2003). AMPK is a mammalian homolog of sucrose non-fermentable protein kinase (SNF-1); it is a member of a serine/threonine protein kinase family. Unlike AMPK, which is activated under various stress conditions resulting in decreased ATP concentrations (Scott *et al.*, 2007), ARKs do not have AMP:ATP ratio-sensitive regulatory subunits. Thus, they do not directly participate in adaptive responses to energy balance (Al-Hakim *et al.*, 2005).

*NUAK1* was first described as supporting AKT-dependent cell survival during nutrient starvation (Suzuki *et al.*, 2003), and has been shown to induce p53 phosphorylation (Hou *et al.*, 2011). *NUAK1* expression is now known to be closely associated with metastases, colorectal cancer and is an indicator of poor prognosis

for glioma (Lu *et al.*, 2013). Recently, it was shown to favor an invasive phenotype in human breast cancer which also depended on AKT signaling. This may be linked to its role in cell adhesion through phosphorylation of the regulatory sub-unit of the myosin light chain 2 (MLC2) phosphatase complex. Other roles for *NUAK1* include: critical role in neurodegenerative diseases; maintenance of metabolic homeostasis; limiting protein synthesis via the mTORC1 signaling pathway; regulating ploidy and senescence via LATS1 kinase. For a general review about regulation and function of the *NUAK* family see (Sun *et al.*, 2013)

Together, *NUAK1* and *NUAK2* inhibit MLC2 phosphatase through three entry points. This complex regulation of MLC2 phosphorylation strictly controls actin stress fiber assembly and contractility,

*Abbreviations used in this paper:* ARK, AMPK-related kinase; HH, Hamburger and Hamilton stage; ISH, *in situ* hybridization; MLC2, myosin light chain 2; NCC, neural crest cell; NLS, nuclear localization signal; NT, neural tube; PFA, para-formaldehyde.

\*Address correspondence to: Jacques Thélu. Univ. Grenoble Alpes, IAB, F-38000 Grenoble, France. Tel: +33-4-76-54-94-32. e-mail: jacques.thelu@ujf-grenoble.fr

<sup>#</sup>Present address: Département de Neurosciences, Centre de Recherche du Centre Hospitalier de l'Université de Montréal (CRCHUM), Montréal, Canada.

Supplementary Material (2 figures) for this paper is available at: <http://dx.doi.org/10.1387/ijdb.140024jt>

Accepted: 10 April 2014. Final, author-corrected PDF published online: 30 September 2014.



probes and imaging of transverse sections, we had detected that expression of *NUAK1* is most prominent throughout the neuroectoderm and that the pattern for *NUAK2* expression suggests a role in remodeling epithelial tissue during head formation.

**Results and Discussion**

**Amino acid sequence alignment**

Comparisons of chick *NUAK1* and *NUAK2* amino acid sequences with homologs from other species reveals high levels of sequence conservation: 80.3% and 64.2% similarity to human sequences and 52.7% and 61.4% similarity to mouse sequence, respectively (Supplementary Fig. S1). Chick *NUAK1* and *NUAK2* are also similar to one another, with an identity score of 52.9%, and 15.0% substitution with a strong degree of conservation (Fig. 1). Like AMPK and other ARKs (except MELK), chick *NUAK1* and *NUAK2* can be phosphorylated by LKB1 on conserved threonine and serine residues (Thr<sup>225</sup>, and Ser<sup>229</sup> on chick *NUAK1*; and Thr<sup>198</sup> and Ser<sup>202</sup> on chick *NUAK2*; highlighted in black, Fig. 1). These residues are part of the conserved T-loop sequences (Kuga *et al.*, 2008) (indicated in yellow and blue, in Fig. 1). The ATP binding sites in the *NUAK* catalytic domain are shown in green and blue in Fig. 1. Unlike *NUAK1*, *NUAK2* is believed to locate to the nucleus (Kuga *et al.*, 2008). This localization is supported by the consensus KKAR nuclear localization signal (NLS) at position 58-

61 (indicated in grey, Fig. 1). Conversely, *NUAK1*, but not *NUAK2*, has a RQRIRS AKT phosphorylation site at position 611-616 in the chick sequence (shown in red, Fig. 1). Evidence suggests that phosphorylation at this site results in protein activation (Suzuki *et al.*, 2003).

***NUAK1* gene expression**

During chick development, *NUAK1* expression was not detected before stage HH6. At this stage, expression was observed in the neural folds (nf), and in the head fold (hf); the primitive streak and Hensen's node were negative (Fig. 2A). Expression increased with development from the head fold stage to head formation (Fig. 2 B-G), with strong expression in the hindbrain region at HH10 (Fig. 2D). Sections at stages HH8-11 show strong expression in the cephalic neural tube (Fig. 3). At stage HH8 in the head forming position, when the neural ridges meet and are beginning to fuse, *NUAK1* was mainly expressed at apical side of epithelial cells located on NT floor (Fig. 3 B-D, B'). The neuroectoderm is a pseudo epithelium with a majority of cells going from basal to apical side, then *NUAK1* mRNA are polarized to the apical pole in these cells. At a more caudal level, where the neural folds splay out, *NUAK1* was mainly expressed at the apical side of all the cells in the groove's walls (Fig. 3E, E'). From the level of the first somite (Fig. 3F), until the caudal primitive fold, no *NUAK1* mRNA was detected in neuroectoderm. At stage HH9, in rostral position, *NUAK1* was

present in neuroectodermal cells, with a slightly higher level at the apical side. In this position, *NUAK1* expression was at low level at roof side (Fig. 3 H-K, H'). Labeling was decreased at a more caudal level (Fig. 3K). The thin black lines in Fig. 3 correspond to shadows due to the thickness of slices. At stage HH11, *NUAK1* expression was reinforced (Fig. 3 M-Q). Neural crest cells (ncc), which migrate laterally from the point where the dorsal neural folds meet, presented only faint or no *NUAK1* expression in whole-mounts (Fig. 3 C,D,H-K,N-Q, asterisk in Fig. 3L). However, we observed a low *NUAK1* expression at somites level (Fig. 3A,F,G,L). The notochord (nc) showed almost no expression (Fig. 3 B-F,I) or only weak expression (Fig. 3 J,O,R). The extra-embryonic regions, area pellucida and area opaca, showed no expression of this gene (Fig. 2 A-D). In contrast, expression was high in the region surrounding the nascent vitelline veins (v) in whole-mount embryos (Fig. 2 C,D), and in sections showing the splanchnic endoderm (Fig. 3 D,E,K). Other endodermal tissue also expressed high levels of *NUAK1*, e.g. in the pharynx (Fig. 3P). In the nascent heart, staining was faint at HH11 (Fig. 3 P,Q), HH12 (Fig. 2E) and HH16 (Fig. 2F) and was no longer detected at HH18 (Fig. 2G).

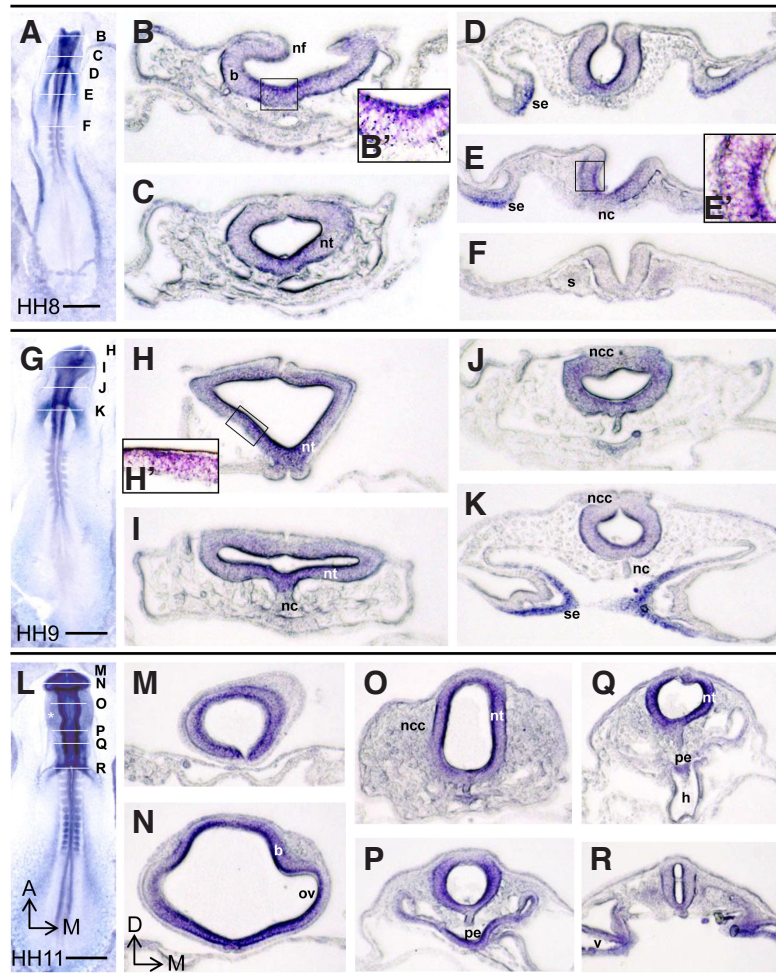


**Fig. 3. *NUAK1* expression pattern in HH8 to HH11 chick embryos.** The position of each section is indicated by white lines in the whole-embryo images (A,G,L). (B',E',H') are zooms of the boxed areas in (B,E,H) showing specific *NUAK1* expression in the neuroectoderm of the head. Migrating NCC express low levels of *NUAK1* in lateral positions (asterisk in L,O). Abbreviations: A-M, anterior-medial; D-M, dorsal-medial; b, brain; h, primordial heart; nc, notochord; ncc, neural crest cells; nf, neural folds; nt, neural tube; ov, optic vesicle; pe, pharyngeal endoderm; s, somite; se, splanchnic endoderm; v, vitelline vein. Scale bar, 500µm.

**NUAK2 gene expression**

*NUAK2* expression was first detected in the rostral region at stage HH6, in the dorsal neural folds and in the head fold region (Fig. 4A). Almost no expression was detected in the primitive streak or Hensen's node itself. In contrast to *NUAK1*, *NUAK2* was extensively expressed in the lateral extra-embryonic domain (Fig. 4A-D). At stages HH7 to HH9, *NUAK2* expression increased in the nascent head and in the spinal cord, while faint

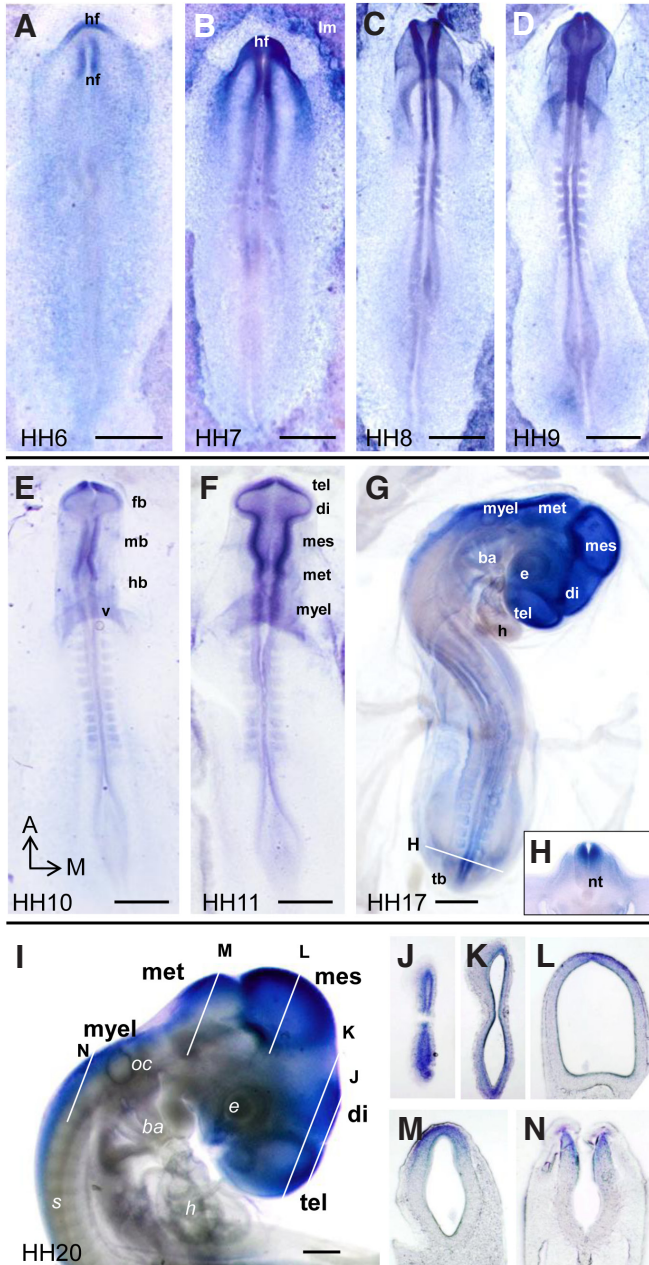


**Fig. 4.** *NUAK2* expression pattern in HH6 to HH17 chick embryos. The position of each section is indicated by white lines in the images (G,I). Abbreviations: A-M, anterior-medial; ba, branchial arch; di, diencephalon; e, eye; fb, forebrain or prosencephalon; h, heart; hb, hindbrain or rhombencephalon; hf, head fold; Im, lateral plate mesoderm; mb, midbrain or mesencephalon; mes, mesencephalon; met, metencephalon; myel, myelencephalon; nf, neural folds; nt, neural tube; oc, otic cup; s, somite; tb, tail bud; tel, telencephalon; v, vitelline vein. Scale bar, 500 $\mu$ m.

labeling was observed in somites (Fig. 4 B-D). At stages HH10 and HH11, neural expression faded except in the telencephalon, the mesencephalon and the rostral half of the metencephalon (Fig. 4 E,F). Very faint expression could be seen in the caudal NT region and in somites (Fig. 4 E,F). At stage HH17, expression was found throughout the encephalon, the eye, the otic cup (Fig. 4G) and in the dorsal NT of the caudal region in transverse sections (Fig. 4H). At stage HH20, expression was restricted to the encephalon, as seen in whole-mounts (Fig. 4I) and sections (Fig. 4 J-N). These sections showed expression to be restricted to the dorsal part of the central nervous system (CNS) this dorsal staining was consistent with that observed in the caudal NT (Fig. 4H). The most anterior section (Fig. 4J) with no cavity shows a strong *NUAK2* expression, this allows us to exclude a potential artifact related to the trapping of purple precipitate in cavities. To definitively exclude this possibility, we also performed negative and positive controls (Supplementary Fig. S2).

Particular attention was paid to *NUAK2* expression in the ectoderm at stages HH7 and HH8 (Fig. 5). During neural groove and head formation, several hinges form successively by curvature of the ectodermic epithelium. The *NUAK2* expression level seems to match this curvature. The first fold is created at the primitive groove (Fig. 5M). *NUAK2* expression was low at the concave medial hinge point (mh) of this fold (black asterisk Fig. 5L) compared to the posterior-most position (Fig. 5N) of the developing embryo, where *NUAK2* is expressed in a roughly flat ectoderm. Fig. 5L showed two additional convex dorsal hinges (dh) with high levels of *NUAK2* mRNA in ectoderm (white asterisk). The intensity of expression and the variation between apico-basal positions in the ectoderm were also observed in other images, especially at positions where the epithelium curves (arrowheads Fig. 5 B'-E'). The convex dh and lateral hinge (lh) at cranial level (Fig. 5 C,G,H) presented high levels of expression. On the other hand, no *NUAK2* expression was detected in the neuroectoderm between the mh and the dh (Fig. 5 B-E,G). The boundary between positive and negative domains located in the neural crest territory (white asterisk in Fig. 5H) is clearly observable (black dashed line Fig. 5H). The mesoderm in axial position, which underlines the medial hinge, expresses *NUAK2* (Fig. 5 C-E).

**Conclusion**

In this paper, we describe the expression patterns for *NUAK1* and *NUAK2* during early chick embryogenesis. We also performed bioinformatics analysis to determine sequence conservation between these two homologs. The expression patterns we describe are similar to those previously obtained for *NUAK1* in wild-type mice embryos using a  $\beta$  Gal fusion protein (Hirano et al., 2006). In the chick, the regionally-restricted expression of *NUAK* isoforms overlaps. Both genes are expressed in the rostral neural folds during head formation, and only very low *NUAK1* and *NUAK2* mRNA expression was detected at the confluence of the neural folds, from where NCC originate. However, specificities did emerge as *NUAK2* was transcribed in the extra-embryonic regions and in the ectoderm of the forming head, while *NUAK1* was not. Conversely, *NUAK1* was transcribed in the neural tube and *NUAK2* was not. At later stages, from HH17 to HH20, *NUAK1* and *NUAK2* have similar expression patterns, largely focused in the brain. This observation leads us to suggest that these two genes have distinct and complementary roles over the course of head development.

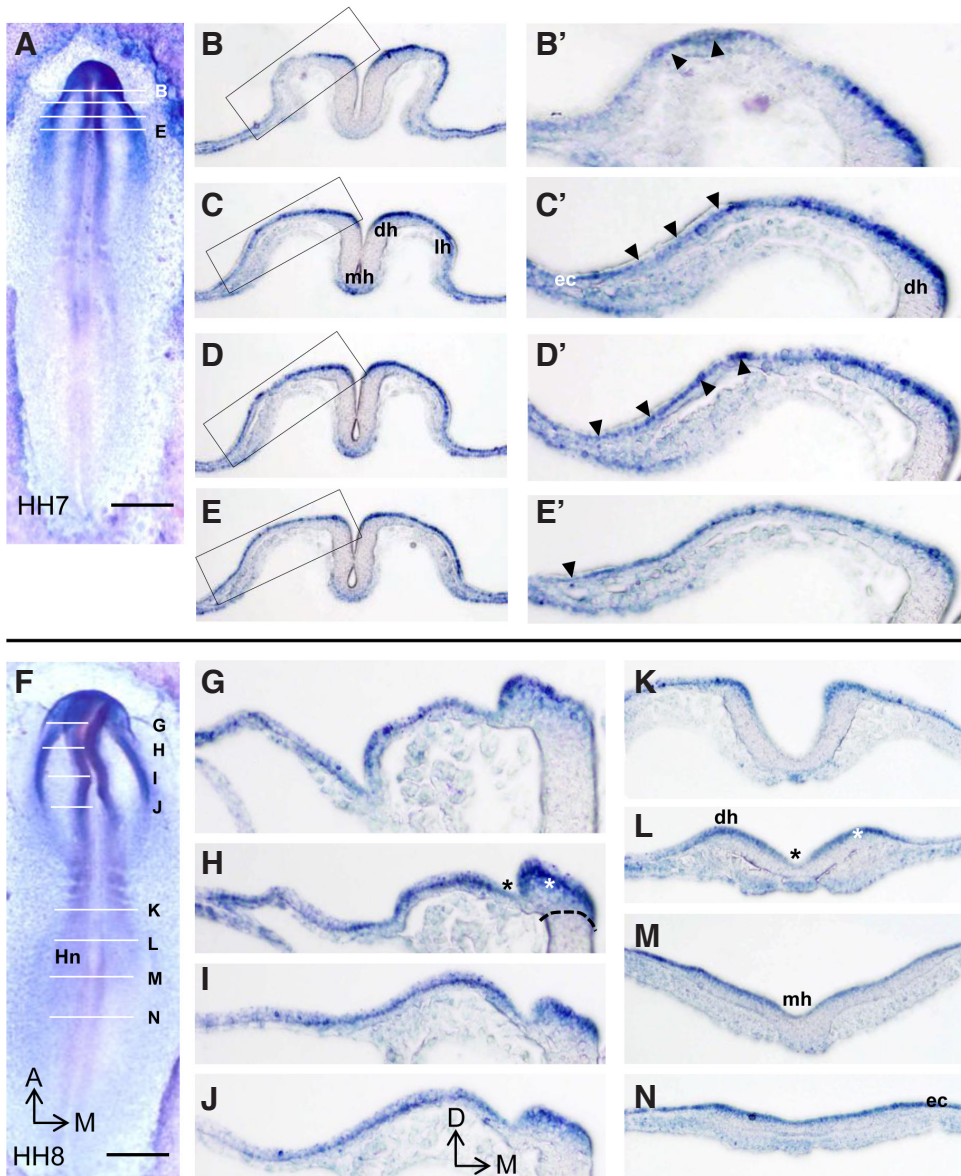


**Fig. 5. *NUAK2* expression at HH7 and HH8 chick embryos.** (B-E) Sections indicated in (A) by white lines. (B' - E') Zooms of the boxed areas in (B - E). (G - N) Sections indicated in (F) by white lines. Black arrow heads indicate variations in the position of *NUAK2* mRNA staining in the ectoderm. Black asterisks indicate low *NUAK2* mRNA levels in ectoderm; white asterisks indicate high *NUAK2* mRNA levels in ectoderm (H,L). In (B' - E') and (G - J), midline is on right side and lateral region is on left side of the images. (H) The positive/negative boundary is underlined with a black dashed line. Abbreviations: A-M, anterior-medial; D-M, dorsal-medial; ec, ectoderm; dh, dorsal hinge point; Hn, Hensen's node; lh, lateral hinge point; mh, median hinge point. Scale bar, 500  $\mu$ m.

This hypothesis is supported by the phenotype of double knock-down mice (Ohmura *et al.*, 2012). Ohmura *et al.*, concluded that *NUAK1* and *NUAK2* have complementary functions in the apical constriction and apico-basal elongation associated with dorsal hinge point formation in the cephalic neural plate during the 5- to 10-somite stages. Interestingly, LKB1, which phosphorylates both *NUAK* homologs, was shown to regulate changes in polarity and adherens junction formation in the *Drosophila* eye (Amin *et al.*, 2008). In addition, *ARK* CG11871 gene (*Drosophila* homolog to mammalian *NUAK*) RNAi experiments revealed developmental defects that partially phenocopy *lkb1* mutants. Altogether, these

observations are consistent with a link between the LKB1/*NUAK* pathway and cell shape. In support of this, we observed a lack or an accumulation of *NUAK2* mRNA in the ectoderm at stages HH7-8, which correlated with concave or convex neural plate curvature. Furthermore, the bending profile of the cephalic ectoderm matches to *NUAK2* mRNA detection in epithelial structures. These observations are clues pointing to a role for *NUAK2* in morphogenesis according to Ohmura *et al.*, (2012). Interestingly, regulation of *NUAK2* expression by a dorsally-derived morphogene (BMPs or Wnts) might also give this type of staining. Furthermore, the expression pattern shown in Fig. 5 K-N suggests repression of the expression of *NUAK2* by a neurogenesis-related ventral signal, such as *Shh* (for a review see Ulloa and Marti, 2010).

## Materials and Methods

### Sequence analysis

The *Gallus gallus* *NUAK* protein sequences were extracted from the NCBI database (<http://www.ncbi.nlm.nih.gov>) as *NUAK1* "XP\_416310.2" and *NUAK2* "XP\_417962.2". Sequence alignment and amino acid identity analysis was performed using the ClustalW algorithm (<http://www.clustal.org>). The positions of putative specific domains were taken from the literature: signature protein kinase ATP-binding regions and LKB1 phosphorylation sites for *NUAK1* (Suzuki *et al.*, 2003) and *NUAK2* (Lefebvre *et al.*, 2001); *NUAK1*-AKT phosphorylation motif (Suzuki *et al.*, 2003); *NUAK2*-nuclear localization signal (NLS) (Kuga *et al.*, 2008).

### Isolation and cloning of *NUAK1* and *NUAK2* probes

Total RNA was isolated from E2 total embryo extracts from chick strain JA957. RNA was reverse transcribed to produce cDNA. Sequence-specific nested primer sets (Table 1) were used to clone partial sequences for both genes (*NUAK1* "Gene ID: 418074" and *NUAK2* "Gene ID: 419828"). An 810 bp PCR product for *NUAK1* and an 830 bp PCR product for *NUAK2* were cloned in TA cloning pGEM-TEasy vectors (Promega). Clones were sequenced using the M13 primer (Beckman Coulter Cogenics). To produce antisense RNA probes, *NUAK1* plasmids were digested with *Nco* I and transcribed with Sp6 RNA polymerase; *NUAK2* plasmids were digested with *Spe* I and transcribed with T7 RNA polymerase and *NUAK2* plasmids were digested with *Apa* I and transcribed with Sp6 RNA polymerase to produce a control sense probe. Digoxigenin (DIG)-labeled RNA antisense and sense probes were transcribed using Roche reagents, according to the manufacturer's instructions. FGF8 plasmids were digested with *Eco* RI and transcribed with T7 RNA polymerase to synthesize an antisense RNA probe used as a positive control (Supplementary Fig. S2).

product for *NUAK1* and an 830 bp PCR product for *NUAK2* were cloned in TA cloning pGEM-TEasy vectors (Promega). Clones were sequenced using the M13 primer (Beckman Coulter Cogenics). To produce antisense RNA probes, *NUAK1* plasmids were digested with *Nco* I and transcribed with Sp6 RNA polymerase; *NUAK2* plasmids were digested with *Spe* I and transcribed with T7 RNA polymerase and *NUAK2* plasmids were digested with *Apa* I and transcribed with Sp6 RNA polymerase to produce a control sense probe. Digoxigenin (DIG)-labeled RNA antisense and sense probes were transcribed using Roche reagents, according to the manufacturer's instructions. FGF8 plasmids were digested with *Eco* RI and transcribed with T7 RNA polymerase to synthesize an antisense RNA probe used as a positive control (Supplementary Fig. S2).

TABLE 1

**NESTED PRIMER SETS USED TO CLONE  
CHICK NUA1 AND NUA2 PROBES**

		Forward primers (5'- 3')	Reverse primers (5'- 3')
NUAK1	Outer set	GCGGCATCACCACAAGCACA	GTGATGCCAATCAATGAACC
	Inner set	CTGCAGGAGACCTTGGGCAA	TGGAGACTCAGAGTCCCTCA
NUAK2	Outer set	CATCGCTACGAGTTCCTGGA	CAAGAAGCACCTCACTTTGG
	Inner set	ATGGGAAGGTGAAGAAAGCA	AAAGAGTGGTGGGAGGAGC

### Embryos and in situ hybridization

Fertilized chick eggs (JA957 strain, SFGA, St Marcellin, France) were incubated at 38°C in a humidified incubator, until embryos reached stage HH6-20, according to the Hamburger and Hamilton table (Hamburger and Hamilton, 1951). Embryos were immediately fixed in ice cold 4% paraformaldehyde (PFA) solution in PBS. They were then dehydrated in a series of methanol baths (25%, 50%, 75%, methanol in PBS), followed by 100% methanol before storing them at -20 °C. The whole-mount *in situ* hybridization protocol was adapted from Wilkinson and Nieto (Wilkinson and Nieto, 1993). Once rehydrated, embryos were loaded into sample holders and subjected to a continuous stream (1.7 ml/min) of successive reagents in an automaton (Flogentec, France) as follows. Samples were washed (15 min) with PBS and 0.1% tween 20 (PBT), then treated with proteinase K (20 µg/ml) in PBT at room temperature (5 to 20 min, depending on embryo size). After washing for 15 min, embryos were post-fixed with 4% PFA solution for 20 min, then washed once again for 15 min. Samples were exposed to hybridization mix (50% formamide; 5x SSC; pH= 4.5; 0.1% tween 20) for 1 hour at 70 °C. A continuous closed-loop-recycling of mRNA probe solution (0.1 µg/ml in hybridization mix) was then applied for 8 hours at 70 °C. Samples were returned to room temperature and treated as follows: 30 min hybridization mix; 1 hour wash; 7 hours closed-loop-recycling of alkaline phosphatase-conjugated anti-hapten antibody (Roche; 1: 3 000); 3 hours wash; and finally, 20 min of Tris-HCl buffer pH= 9.5. The total duration of the protocol was 22 hours. Some solutions, such as probes or antibodies were collected at the end of steps for future use, others were collected for waste treatment. Enzymatic detection was then performed in NBT/BCIP solution (Roche) under constant observation.

### Sections and analysis

After staining, we checked that no signal was observed with sense probes. Embryos were then fixed overnight in 4% PFA, rinsed in PBS and cleared in an 80% glycerol solution in PBS. Embryos were photographed in whole-mounts using an Olympus SZX10 stereomicroscope equipped with DP25 color camera and Cellsens software. Embryos were rinsed for 5 min in PBS, embedded overnight in 7.5% gelatin and 15% sucrose, frozen at -65 °C and sectioned (20 µm) using a LEICA cryomicrotome. Slides were observed under an Olympus BX41 microscope equipped with DP70 color camera and AnaliSiS software. Images were edited using Adobe Photoshop CS4 and Microsoft PowerPoint software.

### Acknowledgements

We thank Maighread Gallagher-Gambarelli for advice relating to language usage and editing. Nicolas Chartier critically reviewed the manuscript. FGF8 plasmids were a kind gift from Sophie Creuzet. The ISH analysis system described in this work was funded in part by Grants-in-aid from Floralis (Grenoble, France), the Gravit innovation fund (Grenoble, France) and the Flogentec Company (Valence, France). Neither of these bodies contributed in any way to study design; data collection, analysis or interpretation; writing the report; or to the decision to submit the article for publication.

### References

- AL-HAKIM, A.K., GORANSSON, O., DEAK, M., TOTH, R., CAMPBELL, D.G., MORRICE, N.A., PRESCOTT, A.R. and ALESSI, D.R. (2005). 14-3-3 cooperates with LKB1 to regulate the activity and localization of QSK and SIK. *J Cell Sci* 118: 5661-5673.
- AMIN, N., KHAN, A., ST JOHNSTON, D., TOMLINSON, I., MARTIN, S., BRENNAN, J. and MCNEILL, H. (2009). LKB1 regulates polarity remodeling and adherens junction formation in the *Drosophila* eye. *Proc Natl Acad Sci USA* 106: 8941-8946.
- EGAN, B. and ZIERATH, J.R. (2009). Hunting for the SNARK in metabolic disease. *Am J Physiol Endocrinol Metab* 296: E969-E972.
- HAMBURGER, V. and HAMILTON, H.L. (1951). A series of normal stages in the development of the chick embryo. *Dev Dyn* 195: 231-272.
- HARDIE, D.G. and ALESSI, D.R. (2013). LKB1 and AMPK and the cancer-metabolism link - ten years after. *BMC Biol* 11: 36.
- HIRANO, M., KIYONARI, H., INOUE, A., FURUSHIMA, K., MURATA, T., SUDA, Y. and AIZAWA, S. (2006). A new serine/threonine protein kinase, Omphk1, essential to ventral body wall formation. *Dev Dyn* 235: 2229-2237.
- HOPPE, P.E., CHAU, J., FLANAGAN, K.A., REEDY, A.R. and SCHRIEFER, L.A. (2010). *Caenorhabditis elegans* unc-82 encodes a serine/threonine kinase important for myosin filament organization in muscle during growth. *Genetics* 184: 79-90.
- HOU, X., LIU, J.E., LIU, W., LIU, C.Y., LIU, Z.Y. and SUN, Z.Y. (2011). A new role of NUA1: directly phosphorylating p53 and regulating cell proliferation. *Oncogene* 30: 2933-2942.
- KUGA, W., TSUCHIHARA, K., OGURA, T., KANEHARA, S., SAITO, M., SUZUKI, A. and ESUMI, H. (2008). Nuclear localization of SNARK; its impact on gene expression. *Biochem Biophys Res Commun* 377: 1062-1066.
- LEFEBVRE, D.L., BAI, Y., SHAHMOLKY, N., SHARMA, M., POON, R., DRUCKER, D.J. and ROSEN, C.F. (2001). Identification and characterization of a novel sucrose-non-fermenting protein kinase/AMP-activated protein kinase-related protein kinase, SNARK. *Biochem J* 355: 297-305.
- LU, S., NIU, N., GUO, H., TANG, J., GUO, W., LIU, Z., SHI, L., SUN, T., ZHOU, F., LI, H. et al. (2013). ARK5 promotes glioma cell invasion, and its elevated expression is correlated with poor clinical outcome. *Eur J Cancer* 49: 752-763.
- MANNING, G., WHYTE, D.B., MARTINEZ, R., HUNTER, T. and SUDARSANAM, S. (2002). The protein kinase complement of the human genome. *Science* 298: 1912-1934.
- NAMIKI, T., TANEMURA, A., VALENCIA, J.C., COELHO, S.G., PASSERON, T., KAWAGUCHI, M., VIEIRA, W.D., ISHIKAWA, M., NISHIJIMA, W., IZUMO, T. et al. (2011). AMP kinase-related kinase NUA2 affects tumor growth, migration, and clinical outcome of human melanoma. *Proc Natl Acad Sci USA* 108: 6597-6602.
- OHMURA, T., SHIOI, G., HIRANO, M. and AIZAWA, S. (2012). Neural tube defects by NUA1 and NUA2 double mutation. *Dev Dyn* 241: 1350-1364.
- SCOTT, J.W., ROSS, F.A., LIU, J.K. and HARDIE, D.G. (2007). Regulation of AMP-activated protein kinase by a pseudosubstrate sequence on the gamma subunit. *EMBO J* 26: 806-815.
- SUN, X., GAO, L., CHIEN, H.Y., LI, W.C. and ZHAO, J. (2013). The regulation and function of the NUA family. *J Mol Endocrinol* 51: R15-22.
- SUZUKI, A., KUSAKAI, G., KISHIMOTO, A., LU, J., OGURA, T., LAVIN, M.F. and ESUMI, H. (2003). Identification of a novel protein kinase mediating Akt survival signaling to the ATM protein. *J Biol Chem* 278: 48-53.
- ULLOA, F. and MARTI, E. (2010). Wnt won the war: antagonistic role of Wnt over Shh controls dorso-ventral patterning of the vertebrate neural tube. *Dev Dyn* 239: 69-76.
- VALLINIUS, T., VAAHTOMERI, K., KOVAC, B., OSICEANU, A.M., VILJANEN, M. and MAKELA, T.P. (2011). An association between NUA2 and MRIP reveals a novel mechanism for regulation of actin stress fibers. *J Cell Sci* 124: 384-393.
- WILKINSON, D.G. and NIETO, M.A. (1993). Detection of messenger RNA by *in situ* hybridization to tissue sections and whole mounts. *Methods Enzymol* 225: 361-373.

**Further Related Reading, published previously in the *Int. J. Dev. Biol.***

**Roles of EphB3/ephrin-B1 in feather morphogenesis**

Sanong Suksaweang, Ting-Xin Jiang, Paul Roybal, Cheng-Ming Chuong and Randall Widelitz  
Int. J. Dev. Biol. (2012) 56: 719-728  
<http://dx.doi.org/10.1387/ijdb.120021rw>

**Skin, cornea and stem cells - an interview with Danielle Dhouailly**

Cheng-Ming Chuong  
Int. J. Dev. Biol. (2009) 53: 775-782  
<http://dx.doi.org/10.1387/ijdb.072552cc>

**Coexpression of *Notch3* and *Rgs5* in the pericyte-vascular smooth muscle cell axis in response to pulp injury**

Henrik Lovschall, Thimios A. Mitsiadis, Knud Poulsen, Kristina H. Jensen and Annette L. Kjeldsen  
Int. J. Dev. Biol. (2007) 51: 715-721  
<http://dx.doi.org/10.1387/ijdb.072393hl>

**Involvement of Hex in the initiation of feather morphogenesis**

Akiko Obinata and Yoshihiro Akimoto  
Int. J. Dev. Biol. (2005) 49: 953-960  
<http://dx.doi.org/10.1387/ijdb.052079ao>

**The Nogent Institute - 50 Years of Embryology**

Nicole Le Douarin  
Int. J. Dev. Biol. (2005) 49: 85-103  
<http://dx.doi.org/10.1387/ijdb.041952nl>

**Mouse-chick neural chimeras**

Josiane Fontaine-Pérus and Yvonnick Chéraud  
Int. J. Dev. Biol. (2005) 49: 349-353  
<http://dx.doi.org/10.1387/ijdb.041943jf>

**Acceleration of early chick embryo morphogenesis by insulin is associated with altered expression of embryonic genes**

Vidya Patwardhan, Madhavi Gokhale and Surendra Ghaskadbi  
Int. J. Dev. Biol. (2004) 48: 319-326  
<http://dx.doi.org/10.1387/ijdb.041844vp>

**Entactin and laminin gamma1-chain gene expression in the early chick embryo**

Nikolas Zagris, Albert E. Chung and Vassilis Stavridis  
Int. J. Dev. Biol. (2005) 49: 65-70  
<http://dx.doi.org/10.1387/ijdb.041812nz>

**5 yr ISI Impact Factor (2011) = 2.959**

